Int. J. Morphol.,
43(5):1530-1536, 2025.

Comparative Study of Tongue and Lingual Papillae in Four Species of Birds: *Otis tarda, Nycticorax nycticorax, Chrysolophus pictus* and *Corvus macrorhynchos*

Estudio Comparativo de la Lengua y las Papilas Linguales en Cuatro Especies de Aves: *Otis tarda, Nycticorax nycticorax, Chrysolophus pictus* y *Corvus macrorhynchos*

Fumei Wang; Wuke Sun; Liwen Zhu & Zhaohui Xie

WANG, F.; SUN, W.; ZHU, L. & XIE, Z. Comparative study of tongue and lingual papillae in four species of birds *Otis tarda*, *Nycticorax nycticorax*, *Chrysolophus pictus*, *Corvus macrorhynchos*. *Int. J. Morphol., 43(5)*:1530-1536, 2025.

SUMMARY: This study examined tongue morphology in four birds (*Otis tarda*, *Nycticorax nycticorax*, *Chrysolophus pictus*, and *Corvus macrorhynchos*) using light and scanning electron microscopy technique. Species-specific variations included mucosal features, papillae patterns, and specialized structures. *Corvus macrorhynchos* showed a bifid tongue tip, marginal filiform papillae, and a symmetrical median groove, with distinct epithelial cell margins. *Nycticorax nycticorax* had clustered filiform papillae and a continuous median sulcus. Lingual gland openings occurred in both body and root regions of *Otis tarda* and *Corvus macrorhynchos* but only at the root in *Nycticorax nycticorax*, while absent in *Chrysolophus pictus*. Histology revealed shared components: keratinized tips, entoglossal cartilage, mucus glands, and root conical papillae. *Nycticorax nycticorax* and *Chrysolophus pictus* uniquely displayed elastic fibers around root blood vessels. All species exhibited posterior-oriented marginal conical papillae, with conserved lamina propria organization despite papillae variations. These differences reflect ecological adaptations. *Corvus macrorhynchos*' bifid tip and *Nycticorax nycticorax*'s clustered papillae suggest dietary specialization, underscoring how avian tongue morphology aligns with environmental niches.

KEY WORDS: Bird; SEM; Histology; Lingual papillae; Lingual glands.

INTRODUCTION

The substantial structural diversity observed in avian oral cavities reflects adaptive strategies corresponding to feeding mechanisms, dietary preferences, and environmental conditions. As a crucial organ in avian feeding behavior, the tongue demonstrates remarkable morphological variations that appear evolutionarily optimized for specific habitat requirements. Key anatomical features warranting particular attention include: the distinctive median sulcus, convex lateral margins, heterogeneous papillae distribution patterns, lingual gland arrangements, and the prominent crest of posterior conical papillae demarcating the tongue's body-root transition. Previous investigations have established significant correlations between lingual architecture and feeding mechanics relative to trophic specialization (Jackowiak & Godynicki, 2005; Emura *et al*., 2008; Al-Zahaby & Elsheikh, 2014). This study systematically examines the morphological adaptations of avian tongues, with particular emphasis on habitat-related anatomical modifications.

This investigation aims to characterize the lingual microarchitecture of four avian species - the Great Bustard (*Otis tarda*), Black-crowned Night Heron (*Nycticorax nycticorax*), Golden Pheasant (*Chrysolophus pictus*), and Jungle Crow (*Corvus macrorhynchos*) - through comparative analysis using scanning electron microscopy (SEM) and light microscopic techniques. While ornithological research has traditionally emphasized ecological distribution, feeding ecology, and reproductive biology (Gao, 2004), recent decades have witnessed growing interest in comparative lingual morphology, with existing literature documenting 78 wild bird species (Erdogan & Iwasaki, 2014). Current understanding suggests strong functional associations between lingual morphology, mucosal epithelial organization, and ecological parameters including feeding strategies and habitat characteristics.

Previous comparative anatomical studies have investigated numerous species, including raptors (*Haliaeetus*

School of Life Science and Bioengineering, Henan University of Urban Construction, Pingdingshan, China.
FUNDED.This work was supported by Baigui Lake Wetland Ecological Monitoring Project (ZC202001).

Received: 2021-04-21 Accepted: 2025-07-20

albicilla, Buteo rufinus), waterfowl (*Anser fabalis*), and various passerines (*Dendrocopos kizuki*, *Corvus corone cornix*), employing both macroscopic and ultrastructural approaches (Iwasaki *et al*., 1997; Jackowiak & Godynicki, 2005; Emura & Chen, 2008; Crole & Soley, 2010). Notably, the selected study species (*O. tarda*, *N. nycticorax*, *C. pictus*, and *C. macrorhynchos*) remain unexamined through SEM methodologies. This research therefore addresses a critical knowledge gap by providing three-dimensional ultrastructural analyses of lingual surfaces, facilitating cross-species comparisons with existing morphological datasets.

MATERIAL AND METHOD

Animal samples. Eight bird cadavers belonging to four different species were included in this study; two bustard (*Otis tarda*), three night heron (*Nycticorax nycticorax*) one golden pheasant (*Chrysolophus pictus*) and two jungle crow (*Corvus macrorhynchos*). The sex of the birds was not considered in this study. The animals died for varies reasons, without timely treatment and were donated by Henan Wildlife Rescue Center. The experimental design adhered to the guidelines of the Animal Ethics Committee of Henan University of Urban Construction (2018).

Gross macroscopic analysis. The oral cavity was opened, and the basal part of the tongue and the mandible was separated. Then, each sample was rinsed five times using 0.9 % physiological NaCl for 5 min each time. Macroscopic observations were carried out on the entire sample with the use of a Sony Alpha 6000L camera. After imaging, the samples were divided into two parts for SEM.

Scanning electron microscopy. The tongues were washed with normal saline and were divided into tissue blocks representing the apex and ventral body and the tongue root. And, after dissection, the tissue samples were fixed in immersion in 2.5 % glutaraldehyde solution, and immerse three times in 0.1 M sodium phosphate buffer (pH 7.0) at 4 °C (3 × 15min). Then, the samples were post-fixed in buffered osmium tetroxide solution at 1 % for 2 h at 4 °C. The samples were rinsed in sodium phosphate buffer (0.1 M, pH 7.0) at 4 °C. Then, samples were dehydrated in a series of alcohol with increasing concentrations starting from 60 % to absolute (50 %, 70 %, 80 %, 90 %, 3×100 %). Because of the size of the tissue blocks, each dehydration step took 15 min. the blocks were then critical point dried in a ALPHA1-2 LD Plus critical point drier. The samples were mounted on aluminum stubs, coated with gold in K550X and examined by SEM apparatus, QUANTA 450.

Light Microscopy. For light microscopy, different parts of the tongues were rapidly set in 10 % neutral-buffered formalin solution for at least 48 h, then dehydrated, transparent and embedded in paraffin wax. 5 µm serial sections were cut transversely and stained with haematoxylin and eosin.

RESULTS

Comparative morphological features of the tongue of birds. The diversity of feeding adaptations among birds is reflected in the form and structure of their tongue (Fig. 1). The tongue is triangular with dagger-like tip and weakly bifid, in the *Otis tarda*; spear-like tongue with sharp tip in the *Nycticorax*

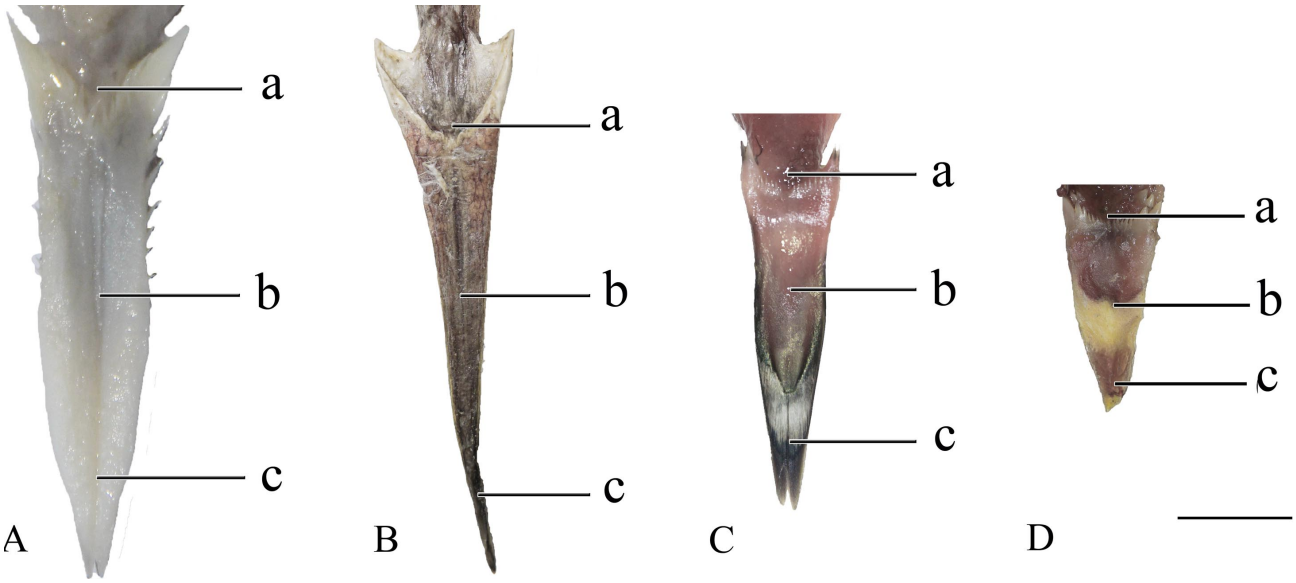

Fig. 1. Macrograph of the tongues. Three parts are distinguished in the tongue: lingual root(a), lingual body(b), lingual apex (c). (A) triangular with dagger-like tip (*Otis tarda*), (B) spear-like tongue with sharp tip (*Nycticorax nycticorax*), (C) bifid apex in tongue (*Corvus macrorhynchos*), (D) wide and shallow triangular with sharp tip (*Chrysolophus pictus*). Bar: 1cm.

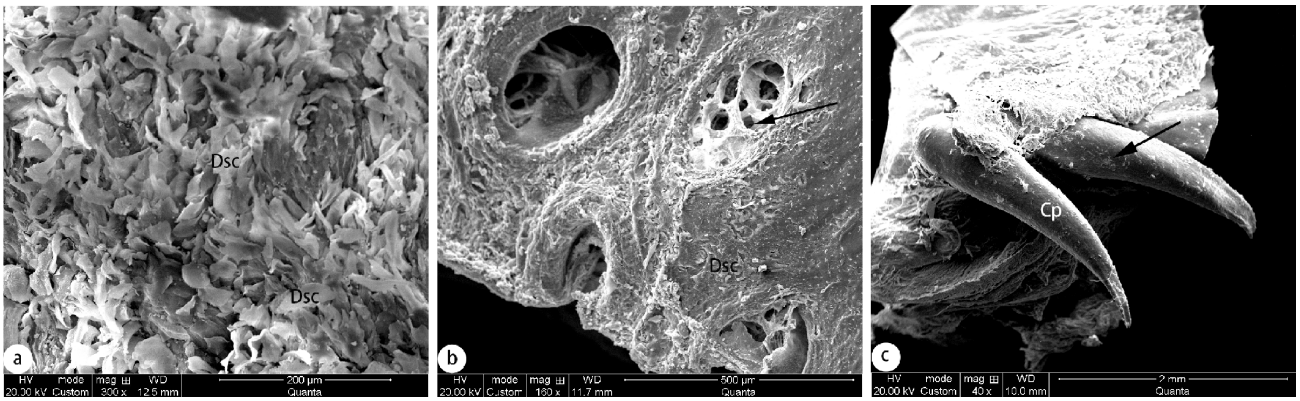

Fig. 2. SEM of the lingual mucosa of the *Otis tarda*. a: There are desquamated superficial epithelial cells of the keratinized epithelium in the lingual apex. Bar: 200 μm; b: surface of the tongue body demonstrating large gland opening which completely fill the mucus (black arrow). Bar: 500 μm; c: SEM image showing two conical papillae, which are curved by caudal direction(arrow). Bar: 2 mm. Dsc, desquamating superficial epithelial cells; Cp, conical papillae; black arrows, orifice of the lingual gland.

nycticorax; elongated with bifid tip in *Corvus macrorhynchos*; wide and shallow triangular with sharp tip in *Chrysolophus pictus*.

Surface features

The lingual mucosa in *Otis tarda.* The target lingual mucosa exhibited distinct morphological variations from the apex to the root (Fig. 2). The mucosa of the lingual apex and body was covered by keratinized squamous epithelium. The apex region lacked papillae and salivary glands. Its surface presented an uneven, lumpy appearance and was composed of epithelium cells with poorly demarcated margins, glands openings and unevenly distributed keratinized cells. In contrast, the tongue body and root contained large, round orifices representing the openings of submucosal mucus-secreting glands, which were filled with mucus. Serrated conical papillae forming a saw-like arrangement were distributed along the root margin, with their apices oriented posteriorly. These papillae measured approximately 2.2 cm in length, featuring rough surfaces covered by keratinized cells with varying degrees of cornification. The peripheral regions were covered by a parakeratinized, multilayered squamous epithelium.

The lingual mucosa in *Nycticorax nycticorax*. The characteristic morphological features observed include a distinct, well-developed median sulcus dividing the mucosal surface into two symmetrical portions from the apex to the body (Fig. 3). At low magnification, the apical region of the lingual mucosa exhibited a superficial layer composed of desquamating squamous epithelial cells with visible intercellular boundaries, demonstrating a complete absence of filiform papillae. The mucosal surface in the body region was uniformly covered by stratified squamous epithelium punctuated by micropores. Conical papillae, measuring approximately 200 μm in diameter, were localized to the lingual root. Numerous glandular openings were distributed

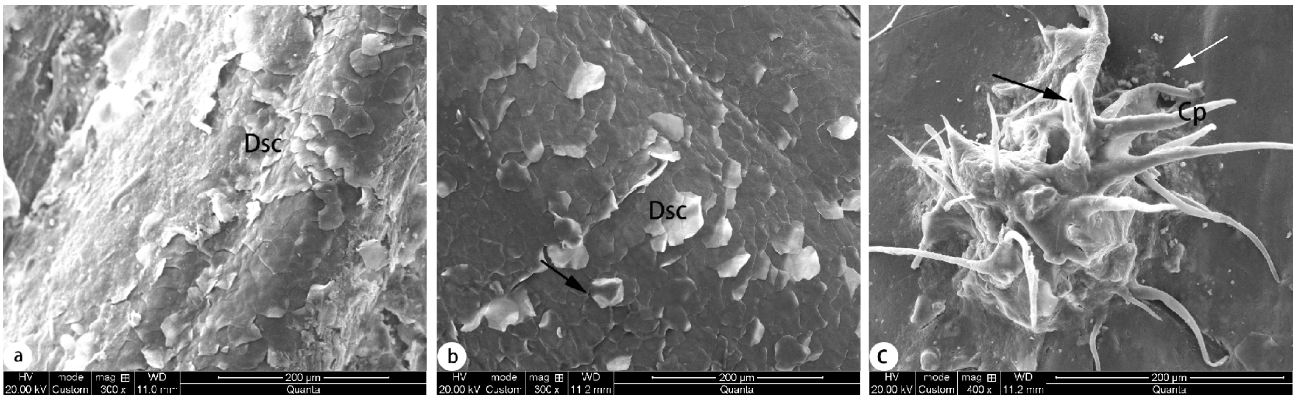

Fig. 3. SEM micrograph of the lingual mucosa of the *Nycticorax nycticorax*. a: the apex of the tongue mucosa showed a surface containing desquamating squamous epithelial cells. b: The surface of the lingual mucosa in the body is covered by the stratified squamous epithelial cells with micro pore (black arrow). Bar: 200 μm; c: shows the filiform papillae with extremity usually bifurcated. Note the openings of salivary glands in the tongue root (black arrow). Bar: 200 μm. Abbreviated labeling as Fig. 1.

throughout both the lingual body and root regions. Filiform papillae occurred in clustered arrangements, with their apical orientations consistently directed posteriorly. The epithelial surface of these papillae displayed distinct non-keratinized characteristics. Both the conical papillae and the lingual root exhibited flattened morphological profiles.

The lingual mucosa in *Corvus macrorhynchos.* The tongue exhibits a dagger-shaped morphology with a bifid tip. A distinctive median groove was observed at the junction between the body and root, dividing the mucosa into two symmetrical, convex lateral structures (Fig. 4). Under low magnification, the apical region of the tongue was lined by desquamating epithelium characterized by a prominent stratum corneum. The desquamating surface further displayed a distinctive tiled pattern of exfoliating cells. Needle-like prominences were distributed along the margins of both body halves, with caudal papillae demonstrating greater size compared to their rostral counterparts. The apex was enveloped by a heavily keratinized, stratified epithelium. Conical papillae at the lingual tip exhibited posteriorly oriented apices. Lingual mucosa in the body region showed desquamating squamous epithelial cells (Dsc) on its surface. These cells displayed distinct intercellular boundaries with clearly demarcated cellular margins. The root mucosa contained mucus-secreting glandular structures, likely functioning to maintain mucosal hydration and prevent desiccation.

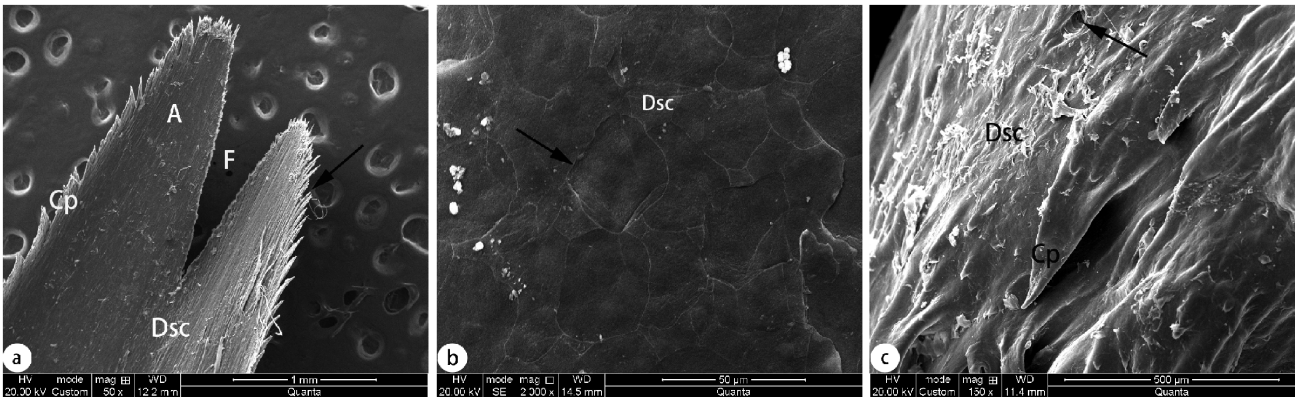

Fig. 4. SEM micrograph of the lingual mucosa of the *Corvus macrorhynchos*. a: The tip is bifid (A, F). the tongue apex was invested by the desquamating epithelium (Dsc). The needle-like prominences (black arrow) were observed distributed along the margin of both halves of the body, and the caudal papillae were larger than the rostral with their extremity curved by caudal direction (Cp). Bar: 1mm; b: SEM image shows desquamate keratinized epithelium (Dsc) in the lingual body. Bar: 50 μm; c: the tongue root was invested by the desquamating epithelium (Dsc). The apices of the conical papillae (Cp)were inclined toward the posterior of the tongue. the many openings (black arrow) of the lingual glands exist in the lingual root. Bar: 500 μm.

The lingual mucosa in *Chrysolophus pictus.* The mucosa of the lingual apex and body is covered by desquamating keratinized stratified squamous epithelium (Fig. 5). Epithelial cells in these regions exhibit poorly demarcated margins. Open mucus-secreting glands are present in both the apex and body. Along the marginal region of the tongue root, a dense row of giant conical papillae (approximately 1-1.5 mm in length) is arranged transversely. The epithelial surface of these papillae displays both keratinized and non-keratinized regions, with the apical portion covered by intensely keratinized multilayered epithelium, occasionally classified as parakeratinized epithelium. The conical papillae of the lingual body are oriented posteriorly. Desquamating surface cells contribute to mechanical protection.

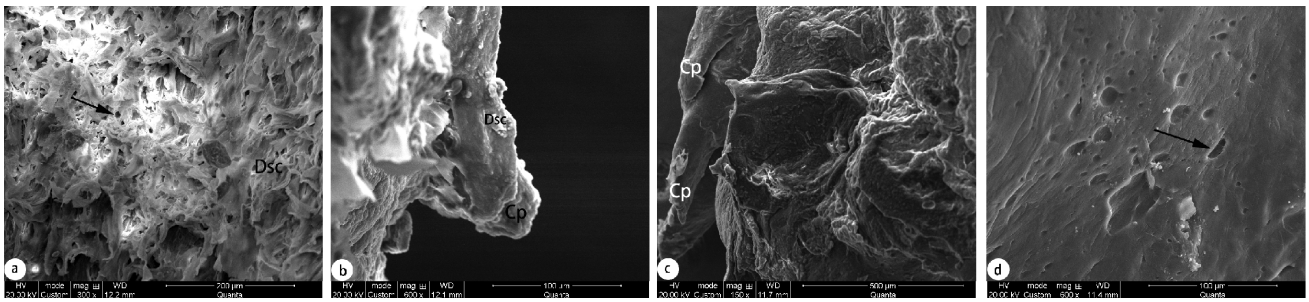

Fig. 5. SEM of the lingual mucosa of the *Chrysolophus pictus*. a: surface containing desquamate keratinized epithelium and the opening of salivary glands in the lingual apex (arrow). Bar: 200 μm; b: Note the conical papillae (Cp). In the marginal region in the papillae were existed desquamate keratinized epithelium (Dsc). Bar:100 μm; c: shows the conical papillae (Cp) with extremity bifurcated. Bar: 500 μm. d: the many openings (arrow) of the lingual glands exist in the lingual root. Bar: 100 μm.

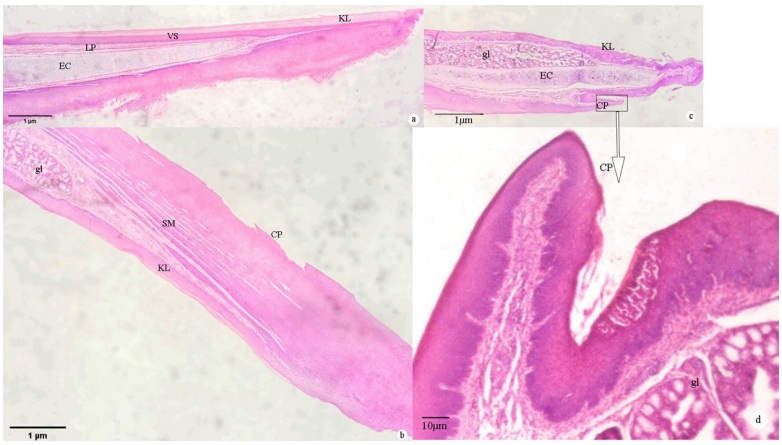

Fig. 6. Photomicrophotographs of the *Otis tarda* tongue showing. a: the thin ventral surface(VS) with thick keratinized layer (KL), the entoglossal cartilage (EC) and lamina propria (LP) on the lingual apex of tongue (HE×4); b: the conical papillae (CP), the lingual mucus gland (gl), the skeletal muscle(SM) and thin keratinized layer (KL) on body of tongue (HE×4); c: root of tongue with mucus gland (gl), keratinized dorsal surface (KL), the entoglossal cartilage (EC) and the conical papillae (CP) (HE×4); d: A higher magnification of Fig (c) showing the conical papillae (CP) and mucus gland (gl) (HE×40).

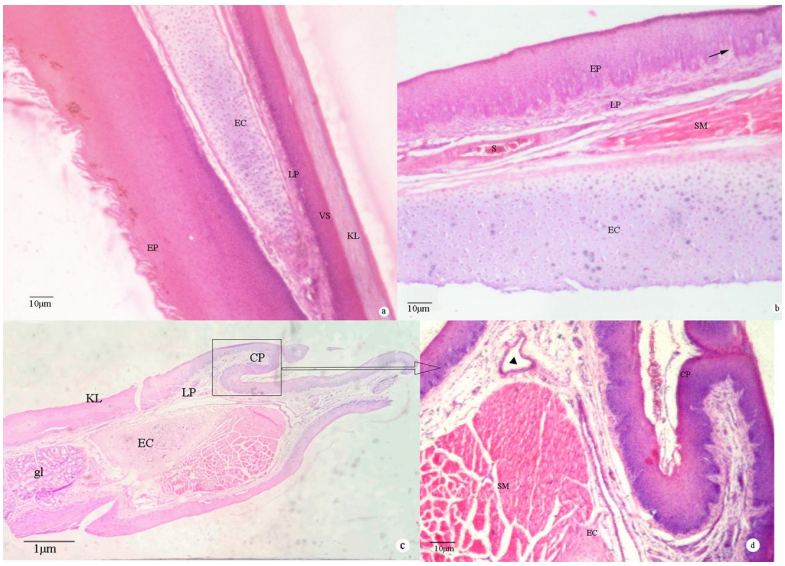

Fig. 7. Photomicrophotographs of the *Nycticorax nycticorax* tongue showing. a: Histomicrograph of the dorsal lingual surface at the apex showing the presence of stratified squamous epithelium (EP), lamina propria (LP), the entoglossal cartilage (EC) and the ventral surface(VS) with keratinized layer (KL) (HE×40); b: Light microscopy of the dorsal surface of the tongue of the body showing thin keratinized layer(KL). Note the presence of stratified squamous epithelium (EP), lamina propria (LP) with its connective tissue core (black arrow) into the papillae and intrinsic skeletal muscle bundles (SM), serous acini (S) and the attached skeletal muscle (SM)(HE×40); c: Histomicrograph of the root of tongue showing the conical papillae(CP), mucus gland (gl), the entoglossal cartilage (EC) and the attached skeletal muscle, mucus gland(gl) and keratinized layer(KL)(HE×4); d: A higher magnification of Fig. (c) showing the conical papillae (CP) and skeletal muscle (SM); the distribution of elastic fibers around the blood vessels (black triangle) (HE×40).

Light Microscope Studies. Histologically, the stratified squamous keratinized epithelium exhibited interspecies variations in thickness and distribution. In the ventral aspect of the lingual apex tip, all four species displayed a thin keratinized layer (Fig. 6a). However, *Nycticorax nycticorax* and *Corvus macrorhynchos* were distinguished by a significantly thicker keratinized epithelium on the dorsal lingual surface at the apex (Figs. 7a, 8a). Distinct histological features were observed in the underlying structures: The lamina propria containing connective tissue cores was specifically identified in *Nycticorax nycticorax* and *Chrysolophus pictus* (Figs. 7b, 9c), whereas *Corvus macrorhynchos* and *Chrysolophus pictus* exhibited entoglossal cartilage integrated with skeletal muscle bundles (Figs. 8b, 9b). Notably, prominent keratinization was observed at the posteriorly inclined conical papillae in three species: *Otis tarda*, *Nycticorax nycticorax*, and *Corvus macrorhynchos* (Figs. 6d, 7d, 8d).

DISCUSSION

The morphological adaptations of avian tongues are closely associated with distinct feeding habits and ecological niches across different environments. Serving crucial roles in food processing and swallowing, these specialized organs demonstrate remarkable structural variations that reflect evolutionary responses to dietary requirements and environmental pressures. Notable examples include the spear-like lingual tip observed in *Nycticorax nycticorax* (Black-crowned Night Heron), a morphological convergence shared with the Japanese pygmy woodpecker (*Dendrocopos kizuki*) as documented by Emura *et al*. (2009b). Contrastingly, *Chrysolophus pictus* (Golden Pheasant) exhibits a bifurcated tongue apex, demonstrating alternative adaptive solutions. Comparative anatomical studies reveal consistent patterns of lingual papilla distribution in *Corvus macrorhynchos* (Large-billed Crow) that align with broader avian trends. The ubiquitous presence of keratinized stratified epithelium across species shows micro-environmental specialization particularly evident in the dorsally flattened keratinized epithelia of lingual apices, a feature similarly observed in *Otus scops*

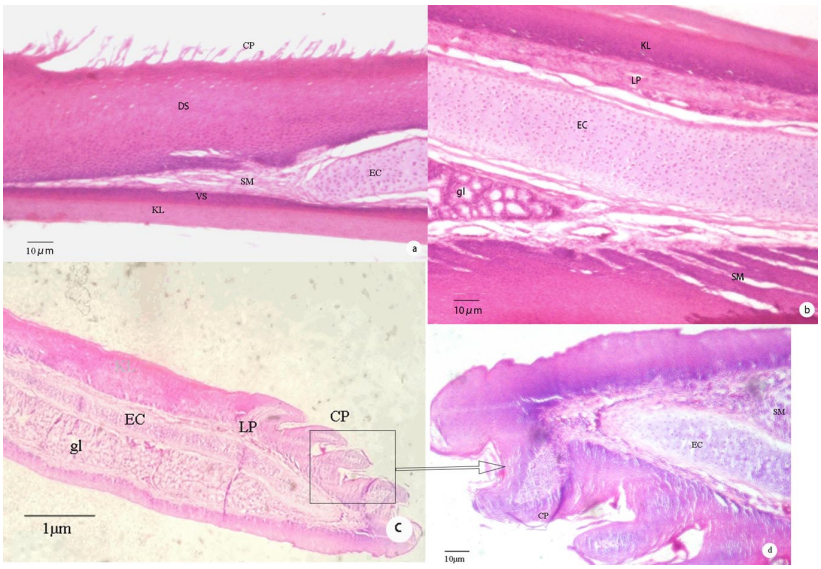

Fig. 8. Photomicrophotographs of the *Corvus macrorhynchos* tongue showing. a: the dorsal surface (DS) and ventral surface (VS) with keratinized layer (KL), the entoglossal cartilage (EC), the conical papillae (CP) and skeletal muscle (SM) on the lingual apex of tongue (HE×40); b: the conical papillae (CP), the lingual mucus gland (gl), the keratinized layer (KL), the entoglossal cartilage (EC) and the attached skeletal muscle (SM) on body of tongue (HE×40); c: root of tongue with mucus gland (gl), lamina propria (LP), the entoglossal cartilage (EC) and the conical papillae (CP) (HE×4); d: A higher magnification of Fig (c) showing the conical papillae (CP) (HE×40).

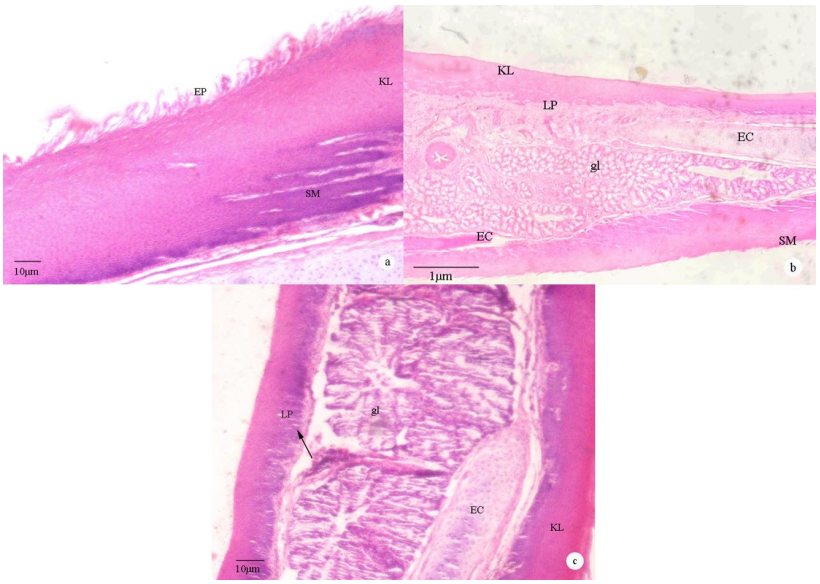

Fig. 9. Photomicrophotographs of the *Chrysolophus pictus* tongue showing. a: the keratinized layer (KL), the stratified squamous epithelium (EP) and skeletal muscle (SM) on the lingual apex of tongue (HE×40); b: the lingual mucus gland (gl), the keratinized layer (KL), the entoglossal cartilage (EC), the lamina propria (LP) and the attached skeletal muscle (SM) on body of tongue(HE×40); c: root of tongue with mucus gland (gl) and the keratinized layer (KL); the presence of lamina propria (LP) with its connective tissue core (black arrow)(HE×40).

(Oriental Scops Owl) by Emura *et al*. (2009a). Current evidence supports a functional correlation between the keratinization patterns of lingual epithelia and trophic specialization, as proposed in the avian feeding mechanism framework by Iwasaki *et al*. (2002).

Variability is also observed in the distribution patterns of conical papillae. *Nycticorax nycticorax* exhibits spiny conical papillae uniformly distributed across the tongue surface, except at the lingual apex and body. In contrast, the tongues of *Otis tarda*, *Corvus macrorhynchos*, and *Chrysolophus pictus* possess sharp, caudally oriented papillae, which are functionally adapted to secure slippery prey. These structures are homologous to the filiform papillae of mammals. Notably, the apical regions of mammalian filiform papillae are softer than their basal counterparts and exhibit caudal curvature (Benetti *et al*., 2009; Burity *et al*., 2009). The crests of conical papillae serve dual functions: facilitating directional transport of ingested material toward the esophagus while preventing regurgitation.

In this study, conical papillae were identified in the lingual root of all four avian species, displaying either rounded or sharply tapered morphologies. Filiform papillae were observed in both the lingual body and root of *Otis tarda* and *Chrysolophus pictus*. Distinctive features of *Corvus macrorhynchos* included bifid-tipped papillae at the lingual apex margin, conical filiform papillae, and polymorphic flat filiform papillae of varying sizes in the lingual root. *Nycticorax nycticorax* demonstrated unique characteristics such as clustered filiform papillae and a prominent median sulcus extending from the apex to the lingual body. These morphological adaptations across species reflect specialized mechanisms for food acquisition, manipulation, and deglutition (Erdogan & Iwasaki, 2014).

We observed that the lingual structures of four bird species exhibit

morphological similarities. The morphological and histological features of mammalian tongues have been shown to reflect differences in mammalian lifestyles and are associated with their respective habitats (Iwasaki, 2002). However, the four avian species examined in this study occupy distinct ecological niches. In Middendorff's Bean Goose (*Anser fabalis* middendorffii), giant conical papillae are arranged in a transverse row between the anterior and posterior lingual regions, while filiform papillae are distributed along the margins of the lingual body (Iwasaki *et al*., 1997). The Jungle Nightjar (*Caprimulgus indicus*) exhibits filiform papillae with posteriorly oriented apices (Emura *et al*., 2010). Similar distributions of filiform papillae on the lingual body have been documented in both owls (Strigiformes) and the Oriental Scops Owl (*Otus sunia*) (Emura & Chen, 2008; Emura *et al*., 2009a). Conversely, distinct differences in lingual papillary distribution were observed among the Great Bustard (*Otis tarda*), Golden Pheasant (*Chrysolophus pictus*), Common Kingfisher (*Alcedo atthis*), Jungle Nightjar (*Caprimulgus indicus*), and Oriental Scops Owl (*Otus sunia*) - species that predominantly feed on reptiles, amphibians, fish, and other vertebrates.

ACKNOWLEDGEMENTS. The authors are grateful to Dajun Deng from Henan Wildlife Rescue Center for his zealous help for the specimen collection. This work was supported by Baigui Lake Wetland Ecological Monitoring Project (ZC202001).

WANG, F.; SUN, W.; ZHU, L. & XIE, Z. Estudio comparativo de la lengua y las papilas linguales en cuatro especies de aves: *Otis tarda*, *Nycticorax nycticorax*, *Chrysolophus pictus* y *Corvus macrorhynchos*. *Int. J. Morphol., 43(5)*:1530-1536, 2025.

RESUMEN: Este estudio examinó la morfología de la lengua en cuatro aves (*Otis tarda*, *Nycticorax nycticorax*, *Chrysolophus pictus* y *Corvus macrorhynchos*) mediante microscopía óptica y electrónica de barrido. Las variaciones específicas de cada especie incluyeron características de la mucosa, patrones de las papilas y estructuras especializadas. *Corvus macrorhynchos* mostró una punta lingual bífida, papilas filiformes marginales y un surco mediano simétrico, con márgenes de células epiteliales definidos. *Nycticorax nycticorax* presentó papilas filiformes agrupadas y un surco mediano continuo. Las aberturas de las glándulas linguales se encontraron tanto en el cuerpo como en la raíz de *Otis tarda* y *Corvus macrorhynchos*, pero solo en la raíz en *Nycticorax nycticorax*, mientras que estaban ausentes en *Chrysolophus pictus*. La histología reveló componentes compartidos: ápices queratinizados, cartílago entogloso, glándulas mucosas y papilas cónicas radiculares. *Nycticorax nycticorax* y *Chrysolophus pictus* mostraron fibras elásticas únicas alrededor de los vasos sanguíneos radiculares. Todas las especies exhibieron papilas cónicas marginales orientadas posteriormente, con una organización de la lámina propia conservada a pesar de las variaciones en las papilas. Estas diferencias reflejan adaptaciones ecológicas. La punta bífida de *Corvus macrorhynchos* y las papilas agrupadas de *Nycticorax nycticorax* sugieren especialización dietética, lo que subraya como la morfología de la lengua aviar se alinea con los nichos ambientales.

PALABRAS CLAVE: Ave; MEB; Histología; Papilas linguales; Glándulas linguales.

REFERENCES

Al-Zahaby, S. A. & Elsheikh, E. H. Ultramorphological and histological studies on the tongue of the common kingfisher in relation to its feeding habit. *J. Basic Appl. Zool., 67(3)*:91-9, 2014.

Benetti, E. J.; Picoli, L. C.; Guimaraes, J. P.; Motoyama, A. A.; Miglino, M. A. & Watanabe, L. S. Characteristics of filiform, fungiform and vallate papillae and surface of interface epithelium-connective tissue of the maned sloth tongue mucosa (*Bradypus torquatus*, Iliger, 1811): light and scanning electron microscopy study. *Anat. Histol. Embryol., 38(1)*:42-8, 2009.

Burity, C. H. F.; da Silva, M. R.; de Souza, A. M.; Lancetta, C. F. F.; Medeiros, M. F. & Pissinatti, A. Scanning electron microscopic study of the tongue in golden-headed lion tamarins, *Leontopithecus chrysomelas* (Callithrichidae: Primates). *Zoologia, 26(2)*:323-7, 2009.

Crole, M. R. & Soley, J. T. Surface morphology of the emu (*Dromaius novaehollandiae*) tongue. *Anat. Histol. Embryol., 39(4)*:355-65, 2010.

Emura, S. & Chen, H. Scanning electron microscopic study of the tongue in the owl (*Strix uralensis*). *Anat. Histol. Embryol., 37(6)*:475-8, 2008.

Emura, S.; Okumura, T. & Chen, H. Scanning electron microscopic study of the tongue in the *Peregrine falcon* and *Common kestrel*. Okajimas *Folia Anat. Jpn., 85(1)*:11-5, 2008.

Emura, S.; Okumura, T. & Chen, H. Scanning electron microscopic study of the tongue in the Oriental scops owl (*Otus scops*). *Okajimas Folia Anat. Jpn., 86(1)*:1-6, 2009a.

Emura, S.; Okumura, T. & Chen, H. Scanning electron microscopic study of the tongue in the Japanese pygmy woodpecker (*Dendrocopos kizuki*). *Okajimas Folia Anat. Jpn., 86(1)*:31-5, 2009b.

Emura, S.; Okumura, T. & Chen, H. Scanning electron microscopic study of the tongue in the Jungle nightjar (*Caprimulgus indicus*). *Okajimas Folia Anat. Jpn., 86(4)*:117-20, 2010.

Erdogan, S. & Iwasaki, S. Function-related morphological characteristics and specialized structures of the avian tongue. *Ann. Anat., 196(2-3)*:75-87, 2014.

Gao, H. Morphological observation of the tongue in some birds. *Chin. J. Zool., 25(5)*:13-6, 2004.

Iwasaki, S. Evolution of the structure and function of the vertebrate tongue. *J. Anat., 201(1)*:1-13, 2002.

Iwasaki, S.; Asami, T. & Chiba, A. Ultrastructural study of the keratinization of the dorsal epithelium of the tongue of Middendorff's bean goose, *Anser fabalis middendorffii* (Anseres, Antidae). *Anat. Rec., 247(2)*:149-63, 1997.

Jackowiak, H. & Godynicki, S. Light and scanning electron microscopic study of the tongue in the white tailed eagle (*Haliaeetus albicilla*, Accipitridae, Aves). *Ann. Anat., 187(3)*:251-9, 2005.

Corresponding author:
Zhaohui Xie
School of Life Science and Bioengineering
Henan University of Urban Construction
Pingdingshan
CHINA

E- mail: xiezhaohui@hncj.edu.cn

Zhaohui Xie https://orcid.org/0000-0001-7878-1079

Fumei Wang https://orcid.org/0009-0000-1634-5335